Module 6: Lecture 17
Deviated Pursuit Guidance Law

Keywords. Deviated pursuit guidance

7.2 Deviated Pursuit Guidance Law

As in the previous section we will carry out a similar analysis for the deviated pursuit guidance law.

7.2.1 The engagement equations

Consider the engagement geometry given in Figure 7.5. Since the missile is using a

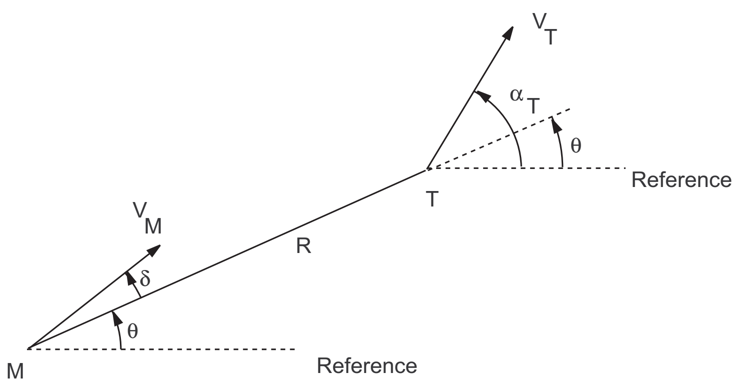

Figure 7.5: *Engagement geometry for deviated pursuit*

deviated pursuit guidance law, at all instants in time, V_M should be directed towards a point that deviates from the current target position by a constant angle δ. This is shown in Figure 7.5. The target is assumed to be a non-maneuvering one. The equations of motion are given by,

$$V_R = \dot{R} = V_T \cos(\alpha_T - \theta) - V_M \cos\delta \qquad (7.26)$$

$$V_\theta = R\dot{\theta} = V_T \sin(\alpha_T - \theta) - V_M \sin\delta \qquad (7.27)$$

Note that here too V_R and V_θ are the two components of the relative velocity between the target and the missile, along the LOS and normal to the LOS. As in the pure pursuit

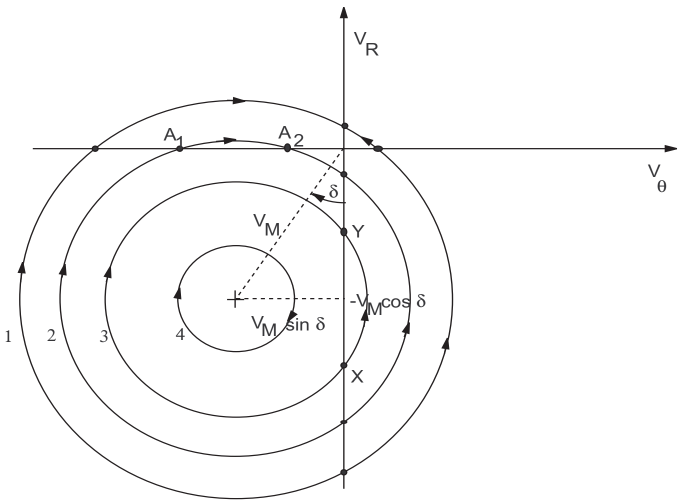

Figure 7.6: *The (V_θ, V_R) trajectories for deviated pursuit with $\delta < \pi/4$*

case, we will first study the behaviour of the relative velocity components.

7.2.2 Trajectory in the (V_θ, V_R)-space

To obtain the engagement trajectory in the (V_θ, V_R)-space let us rewrite (7.26) and (7.27) as,

$$
\begin{aligned}
V_R + V_M \cos\delta &= V_T \cos(\alpha_T - \theta) \\
V_\theta + V_M \sin\delta &= V_T \sin(\alpha_T - \theta)
\end{aligned}
$$

Squaring both equations and summing we obtain,

$$(V_R + V_M \cos\delta)^2 + (V_\theta + V_M \sin\delta)^2 = V_T^2 \tag{7.28}$$

This is the equation of a circle in the (V_θ, V_R)-space with center at $(-V_M \sin\delta, -V_M \cos\delta)$ and radius equal to V_T. It shows that the (V_θ, V_R) point remains on the circumference of this circle as the engagement proceeds. This circle is shown in Figure 7.6 for the case when $\delta < \pi/4$. The arrows in Figure 7.6 denote the direction in which the (V_θ, V_R) point moves from different positions in the (V_θ, V_R)-space with respect to time. These directions are obtained as follows: Differentiating (7.26) and (7.27), we obtain,

$$\dot{V}_R = -V_T \sin(\alpha_T - \theta)(-\dot\theta) = \dot\theta(V_\theta + V_M \sin\delta) \tag{7.29}$$

$$\dot{V}_\theta = V_T \cos(\alpha_T - \theta)(-\dot\theta) = -\dot\theta(V_R + V_M \cos\delta) \tag{7.30}$$

Multiplying R on both sides of both the above equations, we get,

$$R\dot{V}_R = V_\theta(V_\theta + V_M \sin\delta) \quad (7.31)$$

$$R\dot{V}_\theta = -V_\theta(V_R + V_M \cos\delta) \quad (7.32)$$

Since $R > 0$, (7.31) implies that

$$\dot{V}_R > 0 \text{ if } \{V_\theta > 0 \text{ and } V_\theta > -V_M \sin\delta\} \text{ OR } \{V_\theta < 0 \text{ and } (V_\theta < -V_M \sin\delta\}$$
$$\dot{V}_R < 0 \text{ if } \{V_\theta > 0 \text{ and } V_\theta < -V_M \sin\delta\} \text{ OR } \{V_\theta < 0 \text{ and } (V_\theta > -V_M \sin\delta\} \quad (7.33)$$

Analyzing (7.32) we find that,

$$\dot{V}_\theta > 0 \text{ if } \{V_\theta > 0 \text{ and } V_R < -V_M \cos\delta\} \text{ OR } \{V_\theta < 0 \text{ and } V_R > -V_M \cos\delta\}$$
$$\dot{V}_\theta < 0 \text{ if } \{V_\theta > 0 \text{ and } V_R > -V_M \cos\delta\} \text{ OR } \{V_\theta < 0 \text{ and } V_R < -V_M \cos\delta\} \quad (7.34)$$

These two conditions determine the direction of movement of the (V_θ, V_R) point.

The points where the circle cuts the V_R-axis are stationary points since at these points $V_\theta = 0$ and so from (7.29) and (7.30) we see that $\dot{V}_\theta = 0$ and $\dot{V}_R = 0$.

The points on the negative V_R axis correspond to the collision triangle and those on the positive V_R axis correspond to the inverse collision triangle. This collision triangle for deviated pursuit is defined by the requirement that the missile has to always point at an angle deviated by δ from the current LOS, and so is given by that value of α_T that satisfies,

$$V_T \sin(\alpha_T - \theta) = V_M \sin\delta \quad (7.35)$$

and the corresponding $V_R < 0$. There are two possibilities for the collision triangle at the point of interception and these are shown in Figure 7.7. Note that, when $\delta = 0$ (pure pursuit), the first one corresponds to a head-on geometry and the second one corresponds to a tail-chase geometry.

In Figure 7.6 we have shown four circles marked as 1, 2, 3, and 4. They correspond to the following conditions:

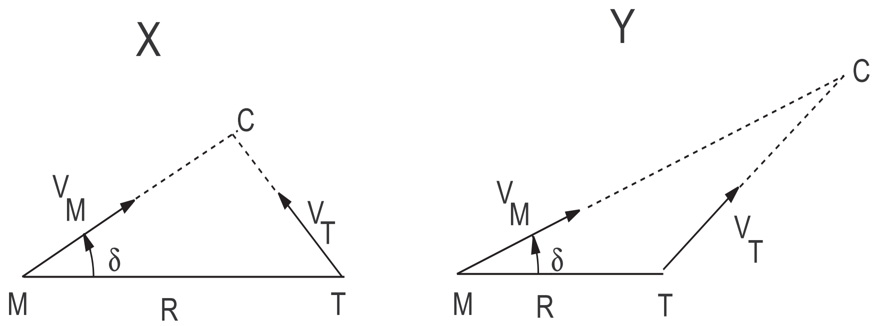

Figure 7.7: *The two possible collision triangles at interception*

$$
\begin{aligned}
1 &: \quad V_T > V_M \\
2 &: \quad V_M \cos\delta < V_T < V_M \\
3 &: \quad V_M \sin\delta < V_T < V_M \cos\delta \\
4 &: \quad V_T < V_M \sin\delta
\end{aligned}
$$

Hence these circles are defined for various values of V_T in relation to V_M and δ. Normally, δ is a small angle and so it is logical to consider $\delta < \pi/4$. However, for the sake of completion we will also consider below the case when $\delta > \pi/4$. The corresponding trajectories are shown in Figure 7.8.

The discussion that follows will be with reference to Figure 7.6 when $\delta < \pi/4$, unless otherwise mentioned.

The largest circle (Circle 1) corresponds to $V_T > V_M$ and, except for those initial conditions which are on the negative V_R axis, all other points end up on the positive V_R axis showing that there is no interception. The miss-distance occurs at the points marked on the figure.

Points corresponding to Circle 2 lead to interception because they end up on the negative V_R axis. However, note that initial conditions in the third quadrant first move into the positive V_R region and then come back to the negative V_R region before hitting the negative V_R axis. Thus, point A1 on the trajectory is the point of closest approach before the missile overshoots the target, turns at point A2, and then intercepts the tar-

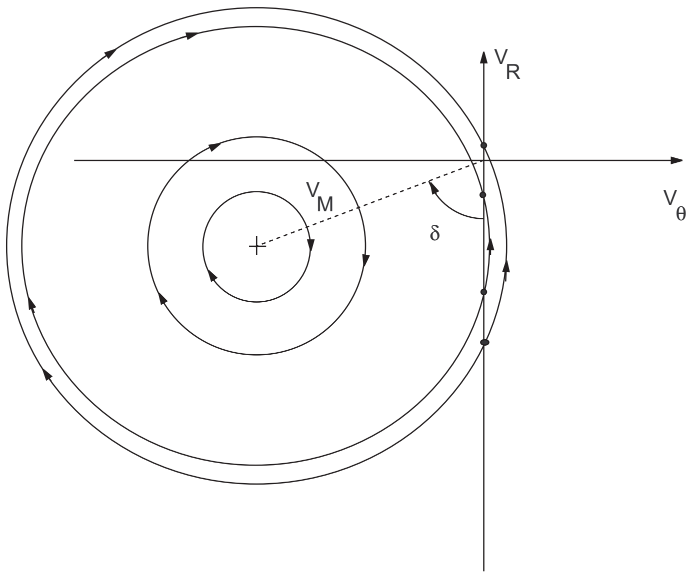

Figure 7.8: *The* (V_θ, V_R) *trajectories for deviated pursuit with* $\delta > \pi/4$

get. A representative trajectory is shown in Figure 7.9.

Points corresponding to Circle 3 also lead to interception, but the trajectory remains in the negative V_R region.

Points corresponding to Circle 4 also lead to interception, but in this case the interception is somewhat different from the previous cases. If we monitor the rate of rotation of the (V_θ, V_R)-point about the center of the circle with respect to time we will

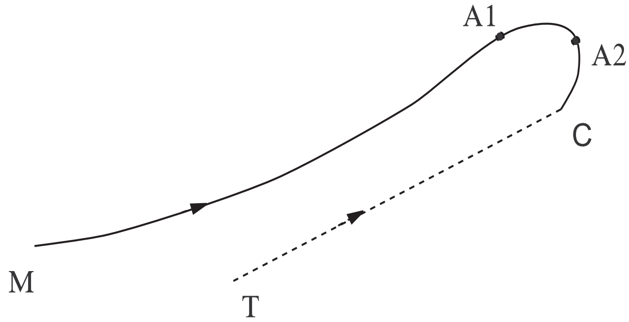

Figure 7.9: *A trajectory corresponding to Circle 2*

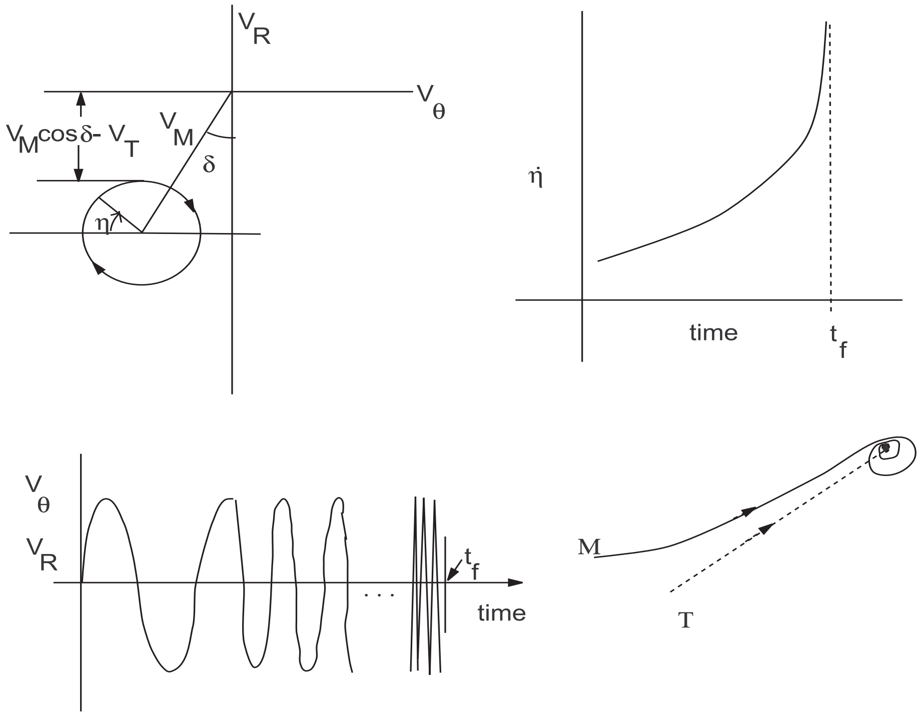

Figure 7.10: *Trajectory and angular velocity for Circle 4*

see that as time increases the angular velocity of this point also increases and tends toward infinity as the time tends to the interception time value. See Figure 7.10. Here, η denotes the angle of the point (V_θ, V_R) from some reference. Then, $|\dot{\eta}| \to \infty$ as $t \to t_f$.

The fact that $|\dot{\eta}| \to \infty$ can be proved by contradiction. Suppose this is not true. Then interception will occur at some definite point on the circle, given by η_f (say) at some finite time t_f. Then, from (7.31) and (7.32), this point will be given by

$$V_{\theta f} = -V_M \sin\delta \tag{7.36}$$

$$V_{rf} = -V_M \cos\delta \tag{7.37}$$

Obviously, since the interception point has to be on the circle, both the above conditions cannot be satisfied. The corresponding missile-target engagement trajectory is such that the missile loops around the target an infinite number of times with smaller and smaller radii till it hits the target. Note that although the missile loops for an infinite number of times it still intercepts at a finite time since the radii of looping reduces with time and becomes zero at t_f. The fact that the interception occurs in finite time can also be seen from Figure 7.10, where it is shown that at any given time instant the value of $V_R \leq -(V_M \cos\delta - V_T)$ and so a finite upper bound on the interception time is given by,

$$t_f \leq \frac{R_0}{V_M \cos\delta - V_T} \tag{7.38}$$